



Preparation and characterization of polyphenylsulfone nanofibrous membranes for the potential use in liquid filtration

S. Kiani^{a,b}, S.M. Mousavi^{a,*}, N. Shahtahmasebi^{c,d}, E. Saljoughi^a

^aFaculty of Engineering, Department of Chemical Engineering, Ferdowsi University of Mashhad, Mashhad, Iran, email: shirin.kiani@stu-mail.um.ac.ir (S. Kiani), Tel./Fax: +98 51 38816840; emails: mmousavi@um.ac.ir (S.M. Mousavi), saljoughi@um.ac.ir (E. Saljoughi)

^bFaculty of Engineering, Membrane Processes and Membrane Research Center, Ferdowsi University of Mashhad, Mashhad, Iran

^cFaculty of Science, Department of Physics, Ferdowsi University of Mashhad, Mashhad, Iran, Tel./Fax: +98 51 38797022; email: Nasser@um.ac.ir

^dNanoresearch Center, Ferdowsi University of Mashhad, Mashhad, Iran

Received 14 March 2015; Accepted 28 July 2015

ABSTRACT

In the present study, polyphenylsulfone (PPSU) nanofibrous membranes were prepared and their potential use in liquid filtration was investigated. The optimum polymer concentration and solvent system for producing beadless fibers were found as 24 wt.% PPSU in N-methyl-2-pyrrolidone/dimethylformamide binary solvent system at a 30:70 volume ratio. The nanofibrous membrane was then heat treated in an oven which resulted in fusion of the fibers at their junction points and also along their length. The untreated and heat-treated membranes were characterized by water contact angle measurement, porosity determination, and tensile tests. Furthermore, performance of the untreated and heat-treated membranes was evaluated by determination of pure water flux and filtration of canned beans production wastewater. The remarkable pure water flux of 7323 L/m² h was observed for the heat-treated membrane as a result of high porosity, improved mechanical stability, and low compaction imposed by the applied heat treatment. The untreated and heat-treated membranes showed 100% turbidity rejection, while chemical oxygen demand and total dissolved solids rejections were 30 and 29% for the untreated membrane and 27 and 25% for the heat-treated one, respectively.

Keywords: Electrospinning; Nanofiber; Filtration; Heat treatment; Polyphenylsulfone

1. Introduction

Electrospinning is a simple and versatile method for fabrication of fibrous mats. The resultant electrospun fiber diameters are usually in the submicrometer range as opposed to conventional fiber spinning techniques where the typical fiber diameters are in the

order of micrometers [1]. In this process, a high voltage is applied to a metallic spinneret in which a polymer solution is passing through. When the voltage reaches a critical value at which the solution charge overcomes the surface tension of the deformed drop of the polymer solution, a jet is produced at the spinneret tip. As the jet travels toward a collector, the

*Corresponding author.

solvent evaporates and the polymer fibers are deposited on the collector [2].

In textile industry and fiber-related scientific literature, the fibers with diameters less than 1,000 nm are generally referred to as nanofibers [3–6]. Nanofibrous mats are notable for their large specific surface area [7,8]. This feature together with their high porosity and interconnected porous structure [7,8] makes the nanofibrous nonwovens as the good candidates for a wide variety of applications such as tissue engineering scaffolds [9], wound dressings [10], sensors [11], catalysts [12], affinity membranes [13], and filtration membranes [8,14].

A variety of polymers, e.g. polysulfones, have been successfully electrospun into nanofibrous mats [5,6,14]. Polysulfones include a class of amorphous thermoplastic polymers characterized by high mechanical strength and supreme thermal resistance [15,16]. Three commercially important polysulfones include polysulfone (PSU), polyethersulfone (PES), and polyphenylsulfone (PPSU) [15]. The repeat units of these polymers are shown in Fig. 1.

Electrospinning of PSU [17–19] and PES [20–24] solutions into nanofibers have been reported in the literature. The PSU or PES electrospun membranes were further modified via heat treatment [18–21], addition of zirconia [22] and titania [24] nanoparticles, oxidation treatment [23], plasma treatment [19], and fiber coating by polydopamine [17] and were applied in liquid filtration. Despite the prevalent use of PSU and PES, PPSU has dominant properties in comparison with the two other polysulfones. Its glass transition temperature is higher than that of PSU and almost equal to that of PES [15,25,26]. The PPSU substantial improvement over PES in hydrolytic stability, impact strength, chemical resistance, and flammability resistance [15] has made it to be considered more recently.

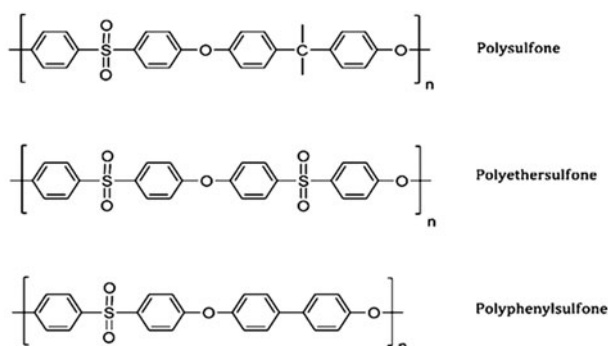


Fig. 1. Repeat units of polysulfone, polyethersulfone, and polyphenylsulfone [15].

With respect to the aforementioned reasons, the objectives of this study were to electrospin PPSU and investigate the effect of parameters including solvent system as well as polymer concentration on morphology of the electrospun nanofibrous membranes. In order to reduce the compaction of the nanofibrous membranes during filtration, a heat treatment was applied and the morphology and mechanical stability before and after the heat treatment were studied. Moreover, porosity, water contact angle, and pure water flux (PWF) of the untreated and heat-treated membranes were determined. Furthermore, the untreated and heat-treated PPSU membranes were applied for treatment of canned beans production wastewater, and their performance was compared.

2. Materials and methods

2.1. Materials

Polyphenylsulfone (PPSU, density = 1.29 g/cm³) was obtained from Sigma-Aldrich. The Mn and Mw approximate range of PPSU measured by gel permeation chromatography based on polystyrene standards were 21,000–23,000 and 53,000–59,000, respectively, which were reported by the supplier. Dimethylformamide (DMF) and N-methyl-2-pyrrolidone (NMP) were supplied from Akkim and Merck, respectively, and used as solvent. All materials were used as received. Wastewater was sampled from a local canned beans production factory. Turbidity, chemical oxygen demand (COD), and total dissolved solids (TDS) of the wastewater were 293 NTU, 2,660, and 1,420 ppm, respectively.

2.2. Electrospinning

PPSU with different concentrations (20, 22, and 24 wt.%) was dissolved in pure NMP, pure DMF, and NMP/DMF mixtures of different volume ratios (20:80, 30:70, and 40:60) by stirring at 30 °C for 12 h to obtain the homogeneous solutions.

The electrospinning apparatus was purchased from Asian Nanostructures Technology Company (ANSTCO), Iran. The polymeric solutions were held in a 10-ml plastic syringe fitted with a needle with an inner diameter of 0.7 mm. The needle was connected to a DC power supply, capable of applying 0–20 kV voltages. During electrospinning, the applied voltage and distance of needle tip to collector were 12 kV and 18.75 cm, respectively. All PPSU solutions were ejected from the syringe at a constant flow rate of 0.4 ml/h. The generated fibers were collected on a grounded collector which was a 5-cm-diameter and 5-cm-long

stainless steel drum, covered with aluminum foil, and rotating at 300 rpm. The linear motion of the collector perpendicular to the drum rotation direction was 220 mm/min resulting an oscillation distance of 4 cm. The operational relative humidity and temperature were kept constant during the experiments at 15–17% and 26–28°C, respectively. The relative humidity and temperature were measured using a digital humidity and temperature sensor (TFA Dostmann/Wertheim).

In order to obtain the nanofibrous membranes for morphological studies in terms of affecting parameters, the electrospinning was performed at the conditions listed in Table 1.

However, preparation of the nanofibrous membranes for water contact angle measurement as well as characterization of porosity, mechanical properties, and filtration performance was carried out by electrospinning of a solution containing 24 wt.% PPSU in NMP/DMF mixture with 30:70 volume ratio. The obtained membranes were kept overnight at room conditions to remove the residual solvents.

2.3. Heat treatment

Post-heat treatment of the prepared membranes was conducted in a SFCN-301 forced convection drying oven (Shinsaeng, Korea) at 245°C for 1 h to increase the structural integrity of the as-spun nanofibers. The membrane was placed in the oven with its sides fixed in order to prevent its shrinkage during heating.

2.4. Scanning electron microscopy

The morphology of electrospun PPSU nanofibrous membranes was investigated by LEO 1,450 VP scanning electron microscope (SEM) made in Germany. Before the SEM characterization, the specimens were sputtered for 2 min by Au-Pd sputter coater (SC7620, England).

Table 1
Electrospinning conditions for morphological studies

No.	PPSU conc. (wt.%)	NMP:DMF vol. ratio
1	24	0:100
2	24	100:0
3	24	20:80
4	24	30:70
5	24	40:60
6	20	30:70
7	22	30:70

2.5. Determination of average fiber diameter, average pore size, and porosity of the electrospun membranes

The fiber diameter distributions and average fiber diameters were determined using Microstructure Image Processing software.

Porosity (ε) of the electrospun membrane was calculated by applying the following equation [14]:

$$\varepsilon = \frac{\rho_0 - \rho}{\rho_0} \times 100\% \quad (1)$$

where ρ_0 and ρ are the density of the polymer used in electrospinning and the apparent density of the nanofibrous membrane, respectively. The electrospun membrane density was determined by measuring the area, thickness, and mass of the specimen. The specimen thickness was measured using a digital outside micrometer (Insize Co.).

The following equation was used for determining the mean pore radius (\bar{r}) of the electrospun membranes [27,28]:

$$\bar{r} = \frac{\sqrt{\pi}}{4} \left(\frac{\pi}{2 \log(\frac{1}{\varepsilon})} - 1 \right) d \quad (2)$$

where ε and d are the porosity and mean fiber diameter of the nanofibrous membrane, respectively.

2.6. Water contact angle measurement

Water contact angle of the nanofibrous membranes was measured by dispensing 40- μ l droplets of distilled water on three different points of the membrane at room temperature. Microscopic images of the droplets were taken using an Olympus DP71 camera mounted on an Olympus SZH10 stereo microscope. The images were then analyzed and the measured angles were averaged and reported.

2.7. Mechanical characterization

Tensile tests were conducted by applying a SANTAM (STM-20, Korea) universal testing machine equipped with a 6 N load cell at room temperature. The tests were performed using the rectangular strips of the membranes with dimensions of 90 mm \times 5 mm at a crosshead speed of 12.5 mm/min.

2.8. Membrane filtration

Permeability of the membranes was studied during water flux measurements using a cross flow cell with

effective membrane area of 12.56 cm². The feed reservoir was put into a water bath to ensure constant temperature of 22°C and filled with 1,000-ml distilled water. The membranes were pre-compacted at trans-membrane pressure of 1.8 bar for 2 h, then the pressure was reduced to 0.6 bar and the water flux was measured every 30 min until obtaining two equal successive measurements. The final water flux was recorded as PWF of the membrane sample, calculated using the following equation [29]:

$$J = \frac{V}{A \Delta t} \quad (3)$$

where V is the permeate volume (L), A is the effective membrane area (m²), and Δt is the sampling time (h).

After determination of PWF, filtration of canned beans production wastewater was performed at trans-membrane pressure of 0.6 bars and temperature of 22°C using 1,000-ml wastewater. Once the filtration process was started, the permeate flux was recorded until it reached a plateau. Then the feed and permeate were sampled and analyzed to determine the values of turbidity, COD, and TDS. The turbidity was determined using Lutron (TU-2016, Taiwan) turbidity meter. COD of the samples was measured using Lovibond (CheckitDirect, Germany) COD photometer. COD tubes were heated in Lovibond (RD125, Germany) thermoreactor at 150°C for 2 h prior to the measurement. An Extech (EC400, USA) conductivity/TDS/salinity meter was applied for determination of the TDS.

To evaluate the filtration efficiency, rejection (R) of the wastewater pollution indices (COD, TDS, and turbidity) was determined using the equation below [30]:

$$R(\%) = 100 \left(1 - \frac{I_p}{I_f} \right) \quad (4)$$

where I_p and I_f are the value of the pollution indices in the permeate and feed, respectively.

3. Results and discussion

3.1. Investigation of the membrane morphology and average fiber diameter

Electrospinning of PPSU nanofibers was studied by varying parameters such as solvent system and polymer concentration. The effect of each parameter on the membrane morphology and average fiber diameter is discussed as follows.

3.1.1. Effect of solvent system

In order to study the effect of solvent system, the properties of each used solvent are required. For DMF and NMP, the boiling points are 153 and 202°C, respectively, and the viscosities at 25°C are 0.82 and 1.8 cP, respectively [31].

Electrospinning of PPSU/DMF solution was unsuccessful because continuous spinning was interrupted by volatility of the solvent, which resulted in rapid evaporation of the solvent and clogging the spinneret before formation of a stable jet [4,32]. Similarly, a proper spinning solution could not be established for NMP. The poor performance of this solvent is attributed to its high boiling point which prevents its sufficient evaporation during electrospinning [33]. When droplets are collected, a different process which is called electrospraying is happening rather than electrospinning [34]. The electrosprayed droplets of PPSU can be seen in Fig. 2.

To achieve the intermediate physical properties, PPSU was dissolved in a binary solvent system of NMP/DMF at different ratios. Fig. 3 represents SEM images and fiber diameter distribution of the electrospun membranes prepared from 24 wt.% PPSU at NMP/DMF volume ratios of 20:80, 30:70, and 40:60, having the corresponding mean fiber diameters of 856, 732, and 872 nm, respectively. Obviously, using mixture of the solvents led to generation of the continuous fibers free of bead. High boiling point of NMP prevented the spinneret from clogging, while the increased solvent evaporation, which was resulted from DMF addition, avoided electrospraying of the solution. Increase in the NMP/DMF ratio from 20:80

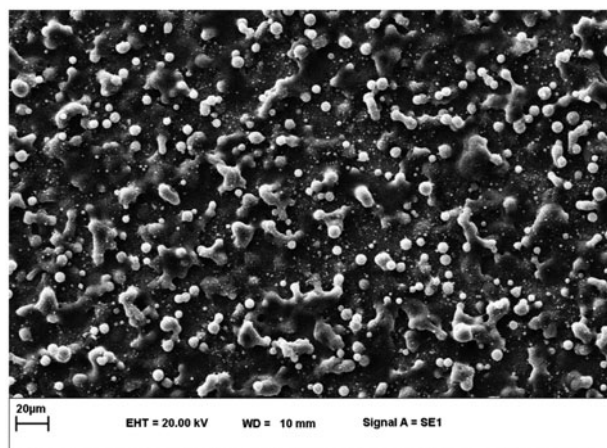


Fig. 2. SEM image of the droplets produced by electro-spraying solution of 24 wt.% PPSU in NMP (magnification: 1,000).

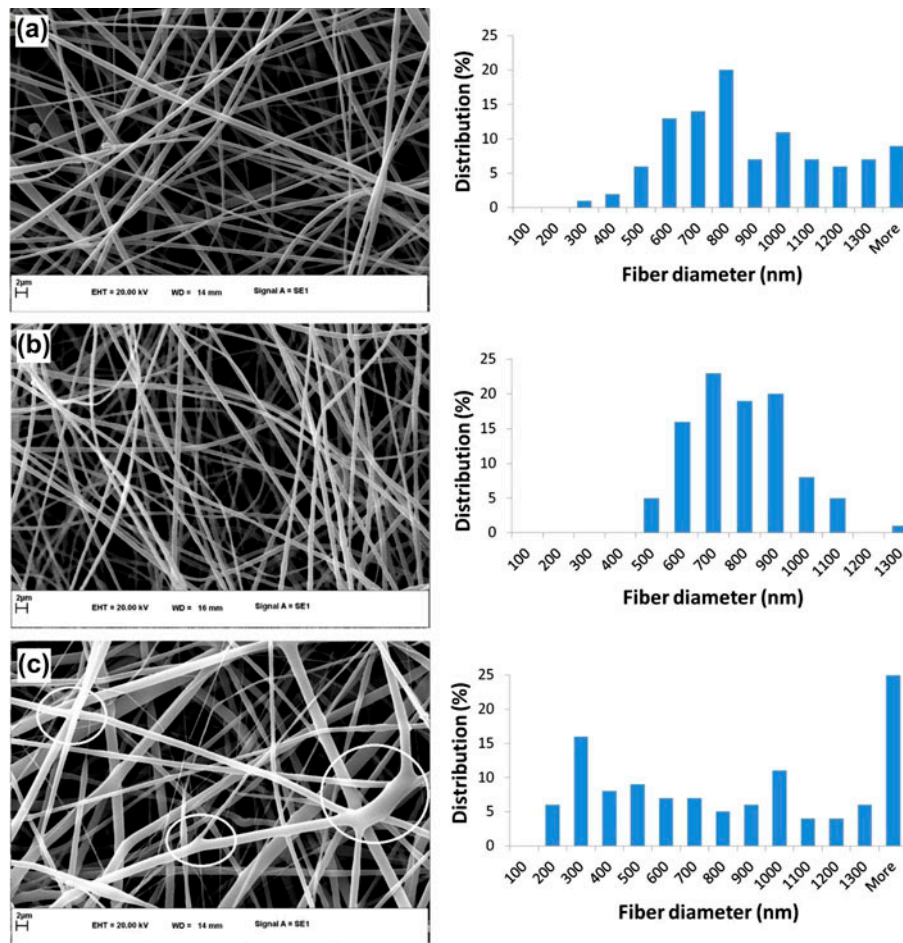


Fig. 3. SEM images and fiber diameter distribution of the electrospun fibrous membranes prepared from 24 wt.% PPSU at NMP/DMF volume ratios of (a) 20:80, (b) 30:70, and (c) 40:60 (magnification: 5,000).

to 30:70 reduced the mean fiber diameter. This can be attributed to higher boiling point of the solution, which provides more time for elongation of the jet as its solidification is slowed down. The enhanced stretching of the solution jet in the electric field results in reduction of mean fiber diameter [35,36]. However, further increase in NMP content increases the solution viscosity, causing higher mean fiber diameter [23]. In addition, increased NMP content in the solvent mixture decreased vapor pressure of the solution. The slow evaporation of NMP caused the fusion of fibers at their junction points as shown in Fig. 3(c) [23].

3.1.2. Effect of polymer concentration

The effect of polymer concentration on morphology and fiber diameter distribution of PPSU fibrous membranes are illustrated in Fig. 4. With respect to the SEM images, at PPSU concentration of 20 wt.%,

there were not enough polymer chain entanglements to allow proper stretching of the solution jet [8,34,37]. Thus, the thin fibers with mean diameter of 173 nm were formed with the presence of almost round-shaped beads. When the polymer concentration was increased to 22 wt.%, the morphology of beads changed from round-shaped to spindle-shaped as a result of enhanced polymer chain entanglements and increased stretching of the jet under the influence of charges [37]. Moreover, diameter of the fibers increased to 216 nm because of increasing viscosity of the solution at higher polymer concentration [34,38]. Increasing the PPSU concentration to 24 wt.% provided enough chain entanglements of the polymer which resulted in formation of the uniform fibers free of bead. However, higher solution viscosity hampered stretching of the jet under electrostatic forces, thus producing fibers with larger mean diameter of 732 nm [34].

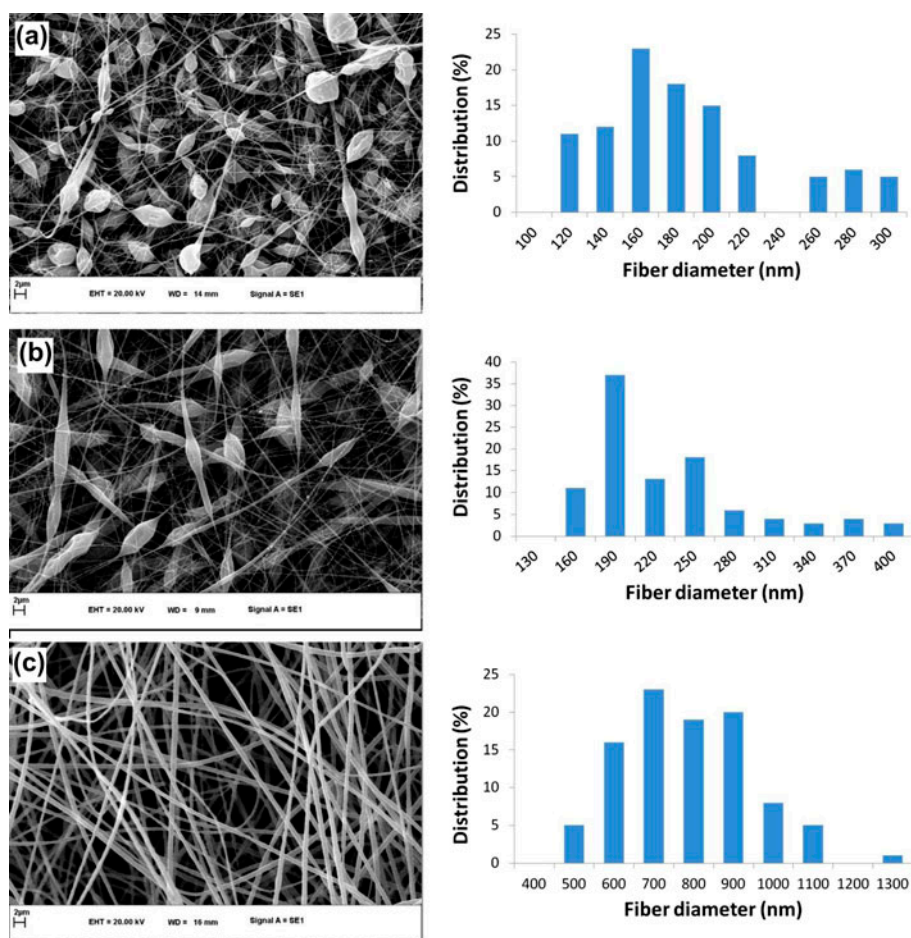


Fig. 4. SEM images and fiber diameter distribution of the electrospun fibrous membranes prepared from (a) 20 wt.% PPSU, (b) 22 wt.% PPSU, and (c) 24 wt.% PPSU at NMP/DMF volume ratio of 30:70 (magnification: 5,000).

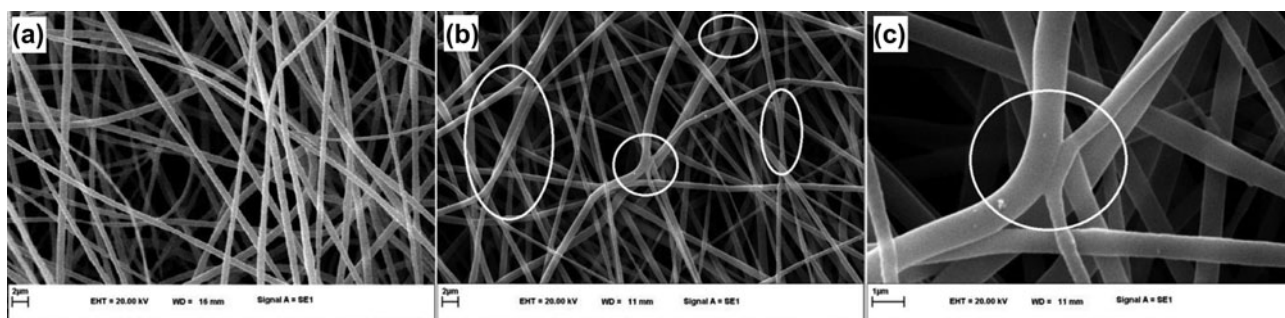


Fig. 5. SEM images of (a) untreated (magnification: 5,000), (b) and (c) heat treated at 245°C for 1 h (magnification: 5,000 and 10,000, respectively) PPSU membranes prepared from 24 wt.% PPSU at NMP/DMF volume ratio of 30:70.

3.2. Effects of heat treatment on the membrane characteristics

For generating a bead-free nanofibrous filtration membrane, the proper conditions were chosen with respect to the results obtained in Section 3.1. Thus, a

solution containing 24 wt.% PPSU in binary solvent of NMP/DMF at 30:70 volume ratio was considered. In order to increase structural integrity of the fibrous membrane, a heat treatment was applied at 245°C for 1 h after electrospinning. The SEM images and fiber

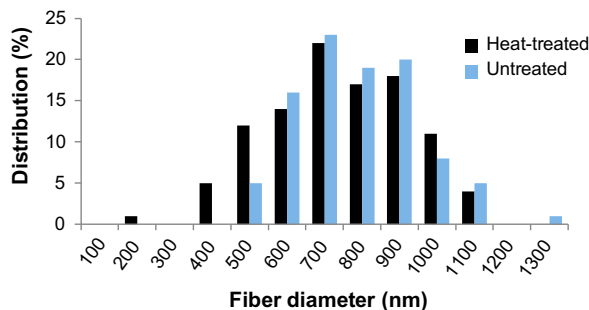


Fig. 6. Fiber diameter distribution of untreated and heat-treated electrospun PPSU membranes.

diameter distribution of the untreated and heat-treated membranes are presented in Figs. 5 and 6, respectively. With respect to the SEM images, the fibers were fused together at their junction points and also along their length after the heat treatment while still maintaining their fibrous structure. The fusion of fibers led to improved structural integrity of the membrane [20,39].

According to Fig. 6, mean fiber diameter of the heat-treated membrane (694 nm) was lower than that of the untreated one (732 nm). During electrospinning, internal stress remains in the fibers which are stretched under electrostatic force. Throughout heating, the polymer molecules tend to rearrange to a stable state. However, since the membrane sides were fixed, an external force was applied. Therefore, rearrangement of molecular chains occurred along the direction of the external force resulting in the fiber diameter reduction [6].

3.2.1. Mean pore size, porosity, and water contact angle of the membranes

Thickness, mean pore radius, porosity, and water contact angle of the untreated and heat-treated membranes are listed in Table 2.

The obtained results show a 67% increase in the membrane thickness after the heat treatment. It should be noted that micrometer measures the membrane thickness in a compacted form due to the applied pressure of the micrometer tip [22]. However, the improved mechanical strength of the heat-treated fibrous membrane gave rise to stability of the

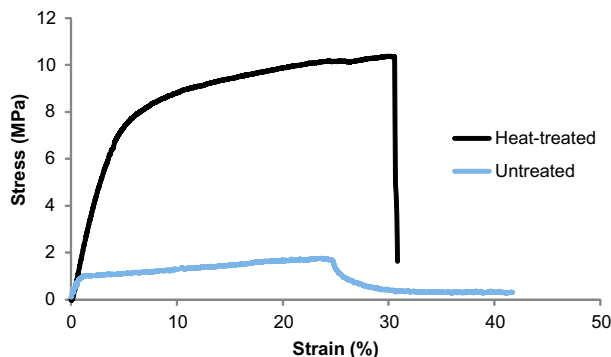


Fig. 7. Stress–strain curves for the untreated and heat-treated membranes.

membrane during determination of the thickness by micrometer, thus resulted in recording higher thickness. Moreover, the aforementioned reason is the dominant cause for the observed increase in the membrane porosity. Mean pore radius of the membranes was calculated according to Eq. (2) and it was noticed that mean pore radius of the heat-treated membrane increased from 3,488 to 4,426 nm.

It is known that water contact angle is the angle between water droplet and an ideal solid surface; however, the contact angle for porous nanofibrous membranes cannot directly be measured. Therefore, for these surfaces, the apparent or macroscopic contact angle is determined, which depends on surface chemistry as well as surface morphology (e.g. roughness) [40]. According to Table 2, water contact angle of the untreated membrane was 131.7° which is in consistency with the hydrophobic nature of electrospun membranes. This characteristic is associated with the inherent surface roughness and trapped air pockets of these membranes [41–43]. Interestingly, the contact angle reduced to 118.4° after the heat treatment. Heat treatment decreases the surface roughness [44]. Lower surface roughness contributes to reduction of the surface hydrophobicity, i.e. lower contact angle [40].

3.2.2. Mechanical properties of the membranes

Mechanical properties of the untreated and heat-treated membranes were examined by tensile test.

Table 2
Properties of the untreated and heat-treated membranes

Membrane	Thickness (μm)	Mean pore radius (nm)	Porosity (%)	Water contact angle ($^\circ$)
Untreated	79	3,488	73.5	131.7
Heat treated	132	4,426	79.1	118.4

Table 3
Mechanical properties of the untreated and heat-treated membranes

Membrane	Elastic modulus (MPa)	Tensile strength at break (MPa)	Elongation at break (%)
Untreated	87.88	1.75	23.71
Heat treated	137.27	10.38	30.22

Table 4
Pure water flux and rejection of pollution indices obtained using the untreated and heat-treated membranes

Membrane	PWF (L/m ² h)	Turbidity rejection (%)	COD rejection (%)	TDS rejection (%)
Untreated	5,058	100	30	29
Heat treated	7,323	100	27	25

Fig. 7 shows the stress–strain curves of PPSU nanofibrous membranes before and after the heat treatment. Regarding this figure for the untreated membrane, the stress increased gradually to the maximum point and then decreased smoothly. On the other hand, for the heat-treated membrane, there was a relatively steep increase in the stress up to the peak and then a rapid drop. Similar results were previously reported for other polymers [5,21,40,45].

The values of elastic modulus, tensile strength at break, and elongation at break for the membranes are presented in Table 3. The heat-treated nanofibrous membrane showed higher elastic modulus, tensile strength at break, and elongation at break as compared to the untreated membrane. Such observations were previously reported for the electrospun poly (vinylidene fluoride) [5,46].

3.2.3. PWF and rejection of the pollution indices

Filtration performance of the untreated and heat-treated membranes was evaluated through PWF measurement as well as treatment of canned beans production wastewater. PWF and rejection of turbidity, COD, and TDS are listed in Table 4. The noticeable value of PWF is the characteristic of nanofibrous membranes because of their high porosity and interconnected pores. The structural integrity and higher mechanical strength of the heat-treated membrane, which was previously proved by the SEM images and tensile test, gave rise to its lower compaction and thus higher porosity during filtration. This feature together with larger pore radius of the heat-treated membrane in comparison with the untreated one resulted in higher PWF.

According to the rejection values reported in Table 4, both of the membranes exhibited almost

similar results. Turbidity rejection of 100% was achieved by the untreated and heat-treated membranes, which implies proper removal of the wastewater suspended solids. It should be noted that screening is not the only mechanism involved in removal of the wastewater pollutants in the present study. Otherwise, most of the pollutants would have passed through the membrane because of the high pore radius resulting in very low rejection values. In fact, separation of pollutants using nanofibrous membranes occurs through a combination of screening and depth filtration [44]. In the latter, the particles are adsorbed to the nanofibers by several mechanisms such as direct interception, inertial compaction, and diffusion (Brownian motion) [18,22]. The entrapped particles initiate the formation of a cake layer within the membrane which starts at the depth of the membrane and grows to the surface [14,22].

The slightly higher COD and TDS rejection obtained using the untreated membrane is a result of its lower porosity intensified during the filtration process due to the low mechanical stability and consequently higher tendency for compaction. A more compacted structure gives rise to the entrapment of more contaminants.

4. Conclusion

In this research, PPSU nanofibrous membranes were prepared and characterized. In the first step, the effect of parameters such as solvent system and polymer concentration on morphology and fiber diameter distribution of electrospun PPSU membranes were investigated. The optimum conditions including the PPSU concentration of 24 wt.% and binary solvent system of NMP/DMF at a 30:70 volume ratio were applied to electrospin beadless PPSU nanofibrous

membrane with mean fiber diameter of 732 nm. The nanofibrous membrane was heated at 245°C to allow fusion of the fibers and improve its structural integrity. In comparison with the untreated membrane, slightly thinner fibers, improved mechanical properties, lower water contact angle, increased porosity, and higher mean pore radius were observed for the heat-treated one. Moreover, PWF of the heat-treated membrane was higher than that of the untreated one. The prepared membranes rejected 100% turbidity and 25–30% COD and TDS during filtration of canned beans production wastewater indicating that the membranes are proper for the wastewater pretreatment.

References

- [1] P. Raghavan, D.H. Lim, J.H. Ahn, C. Nah, D.C. Sherrington, H.S. Ryu, H.J. Ahn, Electrospun polymer nanofibers: The booming cutting edge technology, *React. Funct. Polym.* 72 (2012) 915–930.
- [2] R.R. Jose, R. Elia, M.A. Firpo, D.L. Kaplan, R.A. Peattie, Seamless, axially aligned, fiber tubes, meshes, microbundles and gradient biomaterial constructs, *J. Mater. Sci. Mater. Med.* 23 (2012) 2679–2695.
- [3] F.L. Zhou, R.H. Gong, Manufacturing technologies of polymeric nanofibres and nanofibre yarns, *Polym. Int.* 57 (2008) 837–845.
- [4] Y.N. Jiang, H.Y. Mo, D.G. Yu, Electrospun drug-loaded core–sheath PVP/zein nanofibers for biphasic drug release, *Int. J. Pharm.* 438 (2012) 232–239.
- [5] S.S. Choi, Y.S. Lee, C.W. Joo, S.G. Lee, J.K. Park, K.S. Han, Electrospun PVDF nanofiber web as polymer electrolyte or separator, *Electrochim. Acta* 50 (2004) 339–343.
- [6] L. Zhang, L.G. Liu, F.L. Pan, D.F. Wang, Z.J. Pan, Effects of heat treatment on the morphology and performance of PSU electrospun nanofibrous membrane, *J. Eng. Fiber. Fabr.* 7 (2012) 7–16.
- [7] L. Huang, S.S. Manickam, J.R. McCutcheon, Increasing strength of electrospun nanofiber membranes for water filtration using solvent vapor, *J. Membr. Sci.* 436 (2013) 213–220.
- [8] N. Wang, Z. Zhu, J. Sheng, S.S. Al-Deyab, J. Yu, B. Ding, Superamphiphobic nanofibrous membranes for effective filtration of fine particles, *J. Colloid Interface Sci.* 428 (2014) 41–48.
- [9] D.I. Braghirolli, D. Steffens, P. Pranke, Electrospinning for regenerative medicine: a review of the main topics, *Drug Discovery Today* 19 (2014) 743–753.
- [10] S. Shahverdi, M. Hajimiri, M.A. Esfandiari, B. Larijani, F. Atyabi, A. Rajabiani, A.R. Dehpour, A.A. Gharehaghaji, R. Dinarvand, Fabrication and structure analysis of poly(lactide-co-glycolic acid)/silk fibroin hybrid scaffold for wound dressing applications, *Int. J. Pharm.* 473 (2014) 345–355.
- [11] S. Liang, X. He, F. Wang, W. Geng, X. Fu, J. Ren, X. Jiang, Highly sensitive humidity sensors based on LiCl–Pebax 2533 composite nanofibers via electrospinning, *Sens. Actuators, B* 208 (2015) 363–368.
- [12] T. Srisook, T. Vongsetskul, J. Sucharitakul, P. Chaiyen, P. Tangboriboonrat, Immobilization of 3-hydroxybenzoate 6-hydroxylase onto functionalized electrospun polycaprolactone ultrafine fibers: A novel heterogeneous catalyst, *React. Funct. Polym.* 82 (2014) 41–46.
- [13] G. Hong, L. Shen, M. Wang, Y. Yang, X. Wang, M. Zhu, B.S. Hsiao, Nanofibrous polydopamine complex membranes for adsorption of Lanthanum(III) ions, *Chem. Eng. J.* 244 (2014) 307–316.
- [14] F. Hejazi, S.M. Mousavi, Electrospun nanofibrous composite membranes of chitosan/polyvinyl alcohol-polyacrylonitrile: preparation, characterization, and performance, *Desalin. Water Treat.* (In Press).
- [15] H.F. Mark, *Encyclopedia of Polymer Science and Technology*, vol. 4, John Wiley & Sons, New York, NY, 2003.
- [16] S. Darvishmanesh, J.C. Jansen, F. Tasselli, E. Tocci, P. Luis, J. Degève, E. Drioli, B. Van der Bruggen, Novel polyphenylsulfone membrane for potential use in solvent nanofiltration, *J. Membr. Sci.* 379 (2011) 60–68.
- [17] L. Huang, J.T. Arena, S.S. Manickam, X. Jiang, B.G. Willis, J.R. McCutcheon, Improved mechanical properties and hydrophilicity of electrospun nanofiber membranes for filtration applications by dopamine modification, *J. Membr. Sci.* 460 (2014) 241–249.
- [18] R. Gopal, S. Kaur, C.Y. Feng, C. Chan, S. Ramakrishna, S. Tabe, T. Matsuura, Electrospun nanofibrous polysulfone membranes as pre-filters: Particulate removal, *J. Membr. Sci.* 289 (2007) 210–219.
- [19] L.T. Choong, Z. Khan, G.C. Rutledge, Permeability of electrospun fiber mats under hydraulic flow, *J. Membr. Sci.* 451 (2014) 111–116.
- [20] S.Sh. Homaeigohar, K. Buhr, K. Ebert, Polyethersulfone electrospun nanofibrous composite membrane for liquid filtration, *J. Membr. Sci.* 365 (2010) 68–77.
- [21] S. Homaeigohar, J. Koll, E.T. Lilleodden, M. Elbahri, The solvent induced interfiber adhesion and its influence on the mechanical and filtration properties of polyethersulfone electrospun nanofibrous microfiltration membranes, *Sep. Purif. Technol.* 98 (2012) 456–463.
- [22] S.S. Homaeigohar, M. Elbahri, Novel compaction resistant and ductile nanocomposite nanofibrous microfiltration membranes, *J. Colloid Interface Sci.* 372 (2012) 6–15.
- [23] K. Yoon, B.S. Hsiao, B. Chu, Formation of functional polyethersulfone electrospun membrane for water purification by mixed solvent and oxidation processes, *Polymer* 50 (2009) 2893–2899.
- [24] S.S. Homaeigohar, H. Mahdavi, M. Elbahri, Extraordinarily water permeable sol–gel formed nanocomposite nanofibrous membranes, *J. Colloid Interface Sci.* 366 (2012) 51–56.
- [25] S. Darvishmanesh, F. Tasselli, J.C. Jansen, E. Tocci, F. Bazzarelli, P. Bernardo, P. Luis, J. Degève, E. Drioli, B. Van der Bruggen, Preparation of solvent stable polyphenylsulfone hollow fiber nanofiltration membranes, *J. Membr. Sci.* 384 (2011) 89–96.
- [26] Y. Liu, X. Yue, S. Zhang, J. Ren, L. Yang, Q. Wang, G. Wang, Synthesis of sulfonated polyphenylsulfone as candidates for antifouling ultrafiltration membrane, *Sep. Purif. Technol.* 98 (2012) 298–307.
- [27] S.J. Eichhorn, W.W. Sampson, Statistical geometry of pores and statistics of porous nanofibrous assemblies, *J. R. Soc. Interface* 2 (2005) 309–318.

- [28] W.W. Sampson, A multiplanar model for the pore radius distribution in isotropic near-planar stochastic fibre networks, *J. Mater. Sci.* 38 (2003) 1617–1622.
- [29] M.A. Haj Asgar Khani, S.M. Mousavi, E. Saljoughi, Cellulose acetate butyrate membrane containing TiO₂ nanoparticle: Preparation, characterization and permeation study, *Korean J. Chem. Eng.* 30 (2013) 1819–1824.
- [30] M. Afifi, H. Alizadeh Golestani, S. Sharifi, S. Kiani, Wastewater treatment of raisins processing factory using micellar-enhanced ultrafiltration, *Desalin. Water. Treat.* 52 (2014) 57–64.
- [31] I.M. Smallwood, *Handbook of Organic Solvent Properties*, Arnold, London, 1996.
- [32] D.G. Yu, W. Chian, X. Wang, X.Y. Li, Y. Li, Y.Z. Liao, Linear drug release membrane prepared by a modified coaxial electrospinning process, *J. Membr. Sci.* 428 (2013) 150–156.
- [33] B. Ghorani, S.J. Russell, P. Goswami, Controlled morphology and mechanical characterisation of electrospun cellulose acetate fibre webs, *Int. J. Polym. Sci.* 2013 (2013) 1–12.
- [34] S. Ramakrishna, K. Fujihara, W.E. Teo, T.C. Lim, Z. Ma, *An Introduction to Electrospinning and Nanofibers*, World Scientific Publishing Co., Singapore, 2005.
- [35] A.Y. Mikheev, I.L. Kanev, T.Y. Morozova, V.N. Morozov, Water-soluble filters from ultra-thin polyvinylpyrrolidone nanofibers, *J. Membr. Sci.* 448 (2013) 151–159.
- [36] Z. Zhao, J. Zheng, M. Wang, H. Zhang, C.C. Han, High performance ultrafiltration membrane based on modified chitosan coating and electrospun nanofibrous PVDF scaffolds, *J. Membr. Sci.* 394–395 (2012) 209–217.
- [37] A. Patanaik, V. Jacobs, R.D. Anandjiwala, Performance evaluation of electrospun nanofibrous membrane, *J. Membr. Sci.* 352 (2010) 136–142.
- [38] S. Kaur, S. Sundarrajan, D. Rana, T. Matsuura, S. Ramakrishna, Influence of electrospun fiber size on the separation efficiency of thin film nanofiltration composite membrane, *J. Membr. Sci.* 392–393 (2012) 101–111.
- [39] Z. Ma, Z. Lan, T. Matsuura, S. Ramakrishna, Electrospun polyethersulfone affinity membrane: Membrane preparation and performance evaluation, *J. Chromatogr. B* 877 (2009) 3686–3694.
- [40] L. Li, R. Hashaikeh, H.A. Arafat, Development of eco-efficient micro-porous membranes via electrospinning and annealing of poly (lactic acid), *J. Membr. Sci.* 436 (2013) 57–67.
- [41] S. Kaur, S. Sundarrajan, R. Gopal, S. Ramakrishna, Formation and characterization of polyamide composite electrospun nanofibrous membranes for salt separation, *J. Appl. Polym. Sci.* 124 (2012) E205–E215.
- [42] S. Sundarrajan, S. Ramakrishna, New directions in nanofiltration applications—Are nanofibers the right materials as membranes in desalination? *Desalination* 308 (2013) 198–208.
- [43] S. Kaur, D. Rana, T. Matsuura, S. Sundarrajan, S. Ramakrishna, Preparation and characterization of surface modified electrospun membranes for higher filtration flux, *J. Membr. Sci.* 390–391 (2012) 235–242.
- [44] M.M.A. Shirazi, A. Kargari, S. Bazgir, M. Tabatabaei, M.J.A. Shirazi, M.S. Abdullah, T. Matsuura, A.F. Ismail, Characterization of electrospun polystyrene membrane for treatment of biodiesel's water-washing effluent using atomic force microscopy, *Desalination* 329 (2013) 1–8.
- [45] S.S. Choi, S.G. Lee, C.W. Joo, S.S. Im, S.H. Kim, Formation of interfiber bonding in electrospun poly (etherimide) nanofiber web, *J. Mater. Sci.* 39 (2004) 1511–1513.
- [46] Y. Liang, S. Cheng, J. Zhao, C. Zhang, S. Sun, N. Zhou, Y. Qiu, X. Zhang, Heat treatment of electrospun Polyvinylidene fluoride fibrous membrane separators for rechargeable lithium-ion batteries, *J. Power Sources* 240 (2013) 204–211.